

# The Effect of Silica Nanoparticles and Carbon Nanotubes on the Toughness of a Thermosetting Epoxy Polymer

T. H. Hsieh,<sup>1</sup> A. J. Kinloch,<sup>1</sup> A. C. Taylor,<sup>1</sup> S. Sprenger<sup>2</sup>

<sup>1</sup>Department of Mechanical Engineering, South Kensington Campus, Imperial College London, London SW7 2AZ, United Kingdom

<sup>2</sup>Nanoresins AG, Charlottenburger Strasse 9, 21502 Geesthacht, Germany

Received 9 April 2010; accepted 6 June 2010

DOI 10.1002/app.32937

Published online 26 August 2010 in Wiley Online Library (wileyonlinelibrary.com).

**ABSTRACT:** Silica nanoparticles and multiwalled carbon nanotubes (MWCNTs) have been incorporated into an anhydride-cured epoxy resin to form “hybrid” nanocomposites. A good dispersion of the silica nanoparticles was found to occur, even at relatively high concentrations of the nanoparticles. However, in contrast, the MWCNTs were not so well dispersed but relatively agglomerated. The glass transition temperature of the epoxy polymer was 145°C and was not significantly affected by the addition of the silica nanoparticles or the MWCNTs. The Young’s modulus was increased by the addition of the silica nanoparticles, but the addition of up to 0.18 wt % MWCNTs had no further significant effect. The addition of both MWCNTs and silica nanoparticles led to a signifi-

cant improvement in the fracture toughness of these polymeric nanocomposites. For example, the fracture toughness was increased from 0.69 MPam<sup>1/2</sup> for the unmodified epoxy polymer to 1.03 MPam<sup>1/2</sup> for the hybrid nanocomposite containing both 0.18 wt % MWCNTs and 6.0 wt % silica nanoparticles; the fracture energy was also increased from 133 to 204 J/m<sup>2</sup>. The mechanisms responsible for the enhancements in the measured toughness were identified by observing the fracture surfaces using field-emission gun scanning electron microscopy. © 2010 Wiley Periodicals, Inc. *J Appl Polym Sci* 119: 2135–2142, 2011

**Key words:** epoxy polymers; multiwalled carbon nanotubes; nanoparticles; silicas; toughness

## INTRODUCTION

Thermosetting epoxy polymers are widely used in fiber composite materials and adhesive applications because of their excellent rigidity, strength, and chemical and thermal resistance. However, these polymers are highly crosslinked and hence are relatively very brittle. Therefore, methods for improving the toughness of such polymers are required, but without degrading their other useful properties. Many ways to toughen thermosets have been discussed in the literature, including the use of rubber [e.g., carboxyl-terminated butadiene-acrylonitrile (CTBN)],<sup>1,2</sup> thermoplastic,<sup>3,4</sup> and inorganic particles.<sup>5,6</sup>

Recently, the addition of nanoparticles has become a well-established route to improve the basic mechanical properties and toughness of thermoset epoxy polymers. Various types of nanoparticle have been used, including silica nanoparticles,<sup>7,8</sup> nanoclays,<sup>9</sup> and carbon nanotubes (CNTs) or nanofibers.<sup>10–13</sup> Kinloch et al.<sup>8</sup> have conducted fracture tests on epoxy polymers modified with silica nanoparticles and reported that their addition resulted in a

significant increase in the toughness of the nanocomposite compared with the unmodified polymer, even at low concentrations of silica nanoparticles. Singh et al.<sup>14</sup> have discussed the effect of filler size on toughness and showed that fillers with a relatively small particle size were indeed more efficient in enhancing the toughening performance. The toughening mechanisms associated with silica nanoparticles in epoxy polymers have been identified by Johnsen et al.<sup>7</sup> and more recently by Hsieh et al.<sup>15</sup> These latter authors also successfully predicted the fracture energy of nanoparticle-modified epoxy polymers and demonstrated that the addition of silica nanoparticles resulted in a greater toughness enhancement than observed for microsized silica particles. Also, nanocomposites using CNTs have been intensively investigated, following the successful synthesis of CNTs in 1991,<sup>16</sup> because CNTs display excellent mechanical and electrical properties. For example, Xie et al.<sup>17</sup> measured the Young’s modulus and tensile strength of CNTs to be 0.45 TPa and 3.6 GPa, respectively, when the CNTs were aligned and synthesized using the chemical vapor deposition method. Also, Falvo et al.<sup>18</sup> used multiwalled carbon nanotubes (MWCNTs) as the tip of the probe of an atomic force microscope (AFM) and showed that the tip consisted of a nanotube that could be subjected to relatively large strains without failure. These studies reveal that CNTs have

Correspondence to: A. C. Taylor (a.c.taylor@imperial.ac.uk).

outstanding material properties, which indicate that they may be able to enhance the mechanical performance of polymer-based nanocomposites. Now, Yeh et al.<sup>11</sup> and Bai<sup>19</sup> have reported that the addition of a low concentration of CNTs led to a significant increase in the Young's modulus and tensile strength of polymeric nanocomposites. Also, Wong et al.<sup>20</sup> have investigated the interface properties of CNT-modified polymers and found that a high interfacial shear stress could be obtained, which was attributed to strong interfacial adhesion between the CNTs and the epoxy polymer. Gojny et al.<sup>21</sup> have investigated the fracture toughness of CNT-based polymeric nanocomposites and concluded that using nanotubes with a high aspect ratio could enhance the fracture toughness. They also showed that the highest value of fracture toughness was obtained when the CNTs were well dispersed in the polymer.

In this study, a series of "hybrid" nanocomposites have been prepared and studied by incorporating both silica nanoparticles and CNTs into an epoxy polymer. The basic mechanical, thermal, and fracture properties of the polymeric nanocomposites have been investigated, and, also, the degree of dispersion of the hybrid nanomodifiers has been examined and the toughening mechanisms investigated.

## EXPERIMENTAL PROCEDURE

### Materials

A diglycidyl ether of bisphenol A (DGEBA) resin, designated "LY-556" from Huntsman (Duxford, UK), with an epoxy equivalent weight (EEW) of 186 g/eq was used. This was cured using a low-viscosity anhydride, "HE 600" from Nanoresins (Geesthacht, Germany) with an amide equivalent weight (AEW) of 170 g/eq. A "hybrid" nanomodified epoxy resin, "R1D1" from Nanoleedge (Quebec, Canada) was used; this consists of 0.36 wt % MWCNTs and 12.28 wt % silica nanoparticles premixed in a DGEBA epoxy resin. Polymeric nanocomposites, with different concentrations of silica nanoparticles and MWCNTs, were formed by blending this "hybrid" nanomodified epoxy resin with silica nanoparticles dispersed in a DGEBA epoxy, i.e., "Nanopox F400" from Nanoresins (Geesthacht, Germany). Also, the silica nanoparticles dispersed in the DGEBA epoxy, i.e., "Nanopox F400," were used as an additional "control" formulation, as no MWCNTs are present in these formulations. All the formulations used in this study are shown in Tables I and II.

### Preparation of nanocomposites

During sample preparation, preprocessing of the "hybrid" nanomodifier was required to achieve a

good dispersion of MWCNTs in the epoxy resin. Following the recommendation of the manufacturer, and after several trials, the following processing was used to form the nanocomposites: the "R1D1" mixture, containing both silica nanoparticles and MWCNTs, was first mixed with the "LY-556" DGEBA resin, using an ultrasonic bath for 2 h and then a mechanical stirrer for 30 min at 50°C. To change the concentrations of the nanomodifiers, a calculated amount of the epoxy resin containing the silica nanoparticles (i.e., the "Nanopox F400") was also added. These processing techniques ensured that all the nanomodifiers were dispersed in the epoxy resin to the optimum level that could be achieved before curing. The mixture was then blended with the anhydride curing agent, using the mechanical stirrer for 20 min at 50°C. The final mixture was degassed at 50°C in a vacuum oven. The resin mixture was then poured into a mould at 50°C; a cure cycle of 100°C for 2 h, followed by a postcure of 10 h at 150°C, was used before cooling down to room temperature.

### Microstructure and thermal properties

AFM studies were undertaken using a "MultiMode" scanning probe microscope from Veeco equipped with a "NanoScope IV controlled J-scanner." A smooth surface was first prepared by cutting the unmodified epoxy polymer and the nanocomposites using a "PowerTome XL" cryo-ultramicrotome from RMC Products. AFM scans were performed in the tapping mode using a silicon probe with a 5 nm tip, and both height and phase images were recorded.

Optical microscopy was performed using slices with a thickness of 100  $\mu\text{m}$ . The slices were cut from plates of the unmodified epoxy polymer and the nanocomposites and then ground and polished to improve the flatness of the surface. The slices were placed on a glass microscope slide and viewed using an "Axio Scope A1 Materials Microscope" from Carl Zeiss.

Differential scanning calorimetry (DSC) was conducted using a cured sample having a mass of about 10 mg, according to the ISO Standard 11357-2,<sup>22</sup> using a "DSC Q2000" from TA Instruments. The sample was tested by using two cycles with a temperature range of 30–180°C at a scanning rate of 10°C/min. The results of the DSC studies were outputted as curves of heat flow versus temperature, in which the glass transition temperature,  $T_g$ , was defined as the inflection point in the second heating cycle.

### Mechanical and fracture tests

The Young's moduli of the unmodified epoxy polymer and the nanocomposites were measured using

uniaxial tensile tests according to ASTM D638.<sup>23</sup> These specimens were prepared by machining samples from 3-mm-thick plates. They had a gauge length of 30 mm with loading end-tabs bonded on at both ends; the end-tabs were made from glass-fiber-reinforced plastic composites and mounted at both ends of the samples using an epoxy adhesive, namely "E32" from Permabond (Eastleigh, UK). The surfaces of the specimens were then polished to remove defects caused by the machining operation. The tensile tests were carried out at 1 mm/min and at 20°C, using a clip-gauge extensometer to measure accurately the displacement of the gauge length. Six replicate tests of the unmodified epoxy polymer and nanocomposite formulations were performed.

The single-edge notch-bend (SENB) test was used to measure the values of toughness of the unmodified epoxy polymer and nanocomposite formulations. The SENB specimens were prepared by machining samples from 6-mm-thick plates, with the dimensions of the specimen in accordance with ASTM Standard D5045.<sup>24</sup> To produce natural cracks, a cooled razor blade was tapped into the end of an initial machined notch. The fracture tests were carried out at a loading rate of 1 mm/min and at 20°C. At least eight replicate tests of each formulation were performed. The fracture energy,  $G_C$ , was calculated using the energy method, and the fracture toughness,  $K_{IC}$ , was calculated using the fracture load. As a cross check, the fracture energy,  $G_C$ , for each material was also calculated from the measured values of  $K_{IC}$  and  $E$  according to the Standard,<sup>25</sup> and good agreement between the values from the two different calculation methods was observed.

### Fractographic studies

To identify the toughening mechanisms that can contribute to an increase in the toughness of the nanocomposites, high-resolution scanning electron microscopy of the fracture surfaces of the SENB specimens was performed using a scanning electron microscope equipped with a field-emission gun (FEG-SEM). A Carl Zeiss "Leo 1525" with a "Gemini" column was used, with a typical accelerating voltage of 5 kV. All specimens were coated with an ~5-nm-thick layer of chromium before imaging.

## RESULTS

### Dispersion of CNTs and silica nanoparticles

The dispersion of the hybrid nanomodifiers was examined using AFM and transmission optical microscopy. The AFM images are shown in Figure 1, with the height difference and the phase (via hard-

ness differences) images shown on the left-hand and right-hand sides, respectively.

The unmodified epoxy is an homogeneous thermoset polymer, see Figure 1(a). When silica nanoparticles alone are added, then these are well dispersed, as can be clearly seen in Figure 1(b). The mean diameter of the silica nanoparticles was measured from this AFM image and found to be 20 nm, as has been observed previously.<sup>15</sup> The AFM images of the nanocomposite containing 0.18 wt % MWNT and 6.0 wt % silica nanoparticles [see Fig. 1(c)] show that the silica nanoparticles are well dispersed, but there are some small agglomerations of the MWCNTs; this was confirmed when FEG-SEM was used to study the fracture surfaces, see below. For example, in the phase image from the AFM studies, shown in Figure 1(c), the silica nanoparticles appear light, and the MWCNT agglomerates appear dark because of the graphitic CNTs. (It should be noted that in the AFM studies, the relative hardness of the phases is reflected in the micrographs of the phase images. However, the relatively soft response of the MWCNT agglomerates, which is apparent, is caused by the AFM probe slipping off the graphitic surface of the nanotubes, rather than reflecting the true hardness of the nanotubes.)

The effect of the nanotube content on the dispersion of the MWCNTs was also investigated by observing 100- $\mu$ m-thick slices using a transmission optical microscope. Figure 2 shows the dispersion of MWCNTs in the nanocomposites, with various concentrations of nanotubes and silica nanoparticles. These micrographs reveal that as the concentration of MWCNTs increases, the size of the agglomerations of the nanotubes becomes larger. In contrast, increasing the concentration of silica nanoparticles does not significantly affect the dispersion of the MWCNTs.

### Mechanical and thermal properties

The measured Young's moduli,  $E$ , of the various formulations are shown in Table I and Figure 3. (In Tables I and II, and the associated Figures, the standard deviations are also quoted.) A modulus of 2.90 GPa was measured for the unmodified epoxy polymer, which is typical for such a polymer.<sup>15</sup> The addition of silica nanoparticles alone to the epoxy polymer leads to a steady increase in the modulus, of up to 3.01 GPa for the formulation containing 6.0 wt % of silica. However, the addition of the MWCNTs only increases slightly the modulus of the hybrid nanocomposites.

DSC was used to investigate the effect of the addition of silica nanoparticles and MWCNTs on the glass transition temperature,  $T_g$ , of the epoxy. The results, shown in Table I, indicate that the  $T_g$  of each formulation is very similar, and that the values are



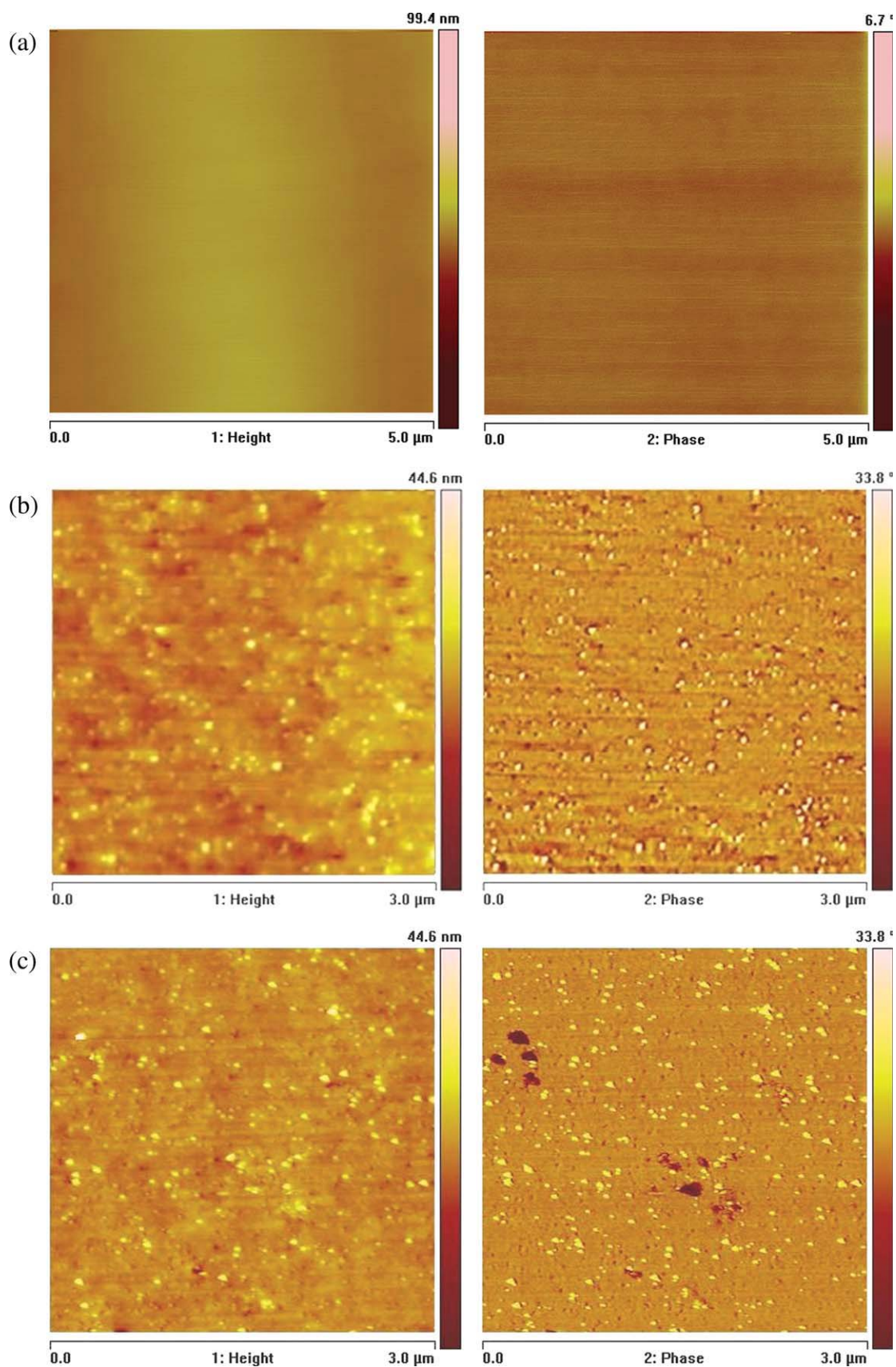


**Figure 1** AFM images of the morphology of the epoxy polymers: (a) unmodified, (b) with 6.0 wt % silica nanoparticles, and (c) with 6.0 wt % silica nanoparticles and 0.18 wt % MWCNTs. [Color figure can be viewed in the online issue, which is available at [wileyonlinelibrary.com](http://wileyonlinelibrary.com).]

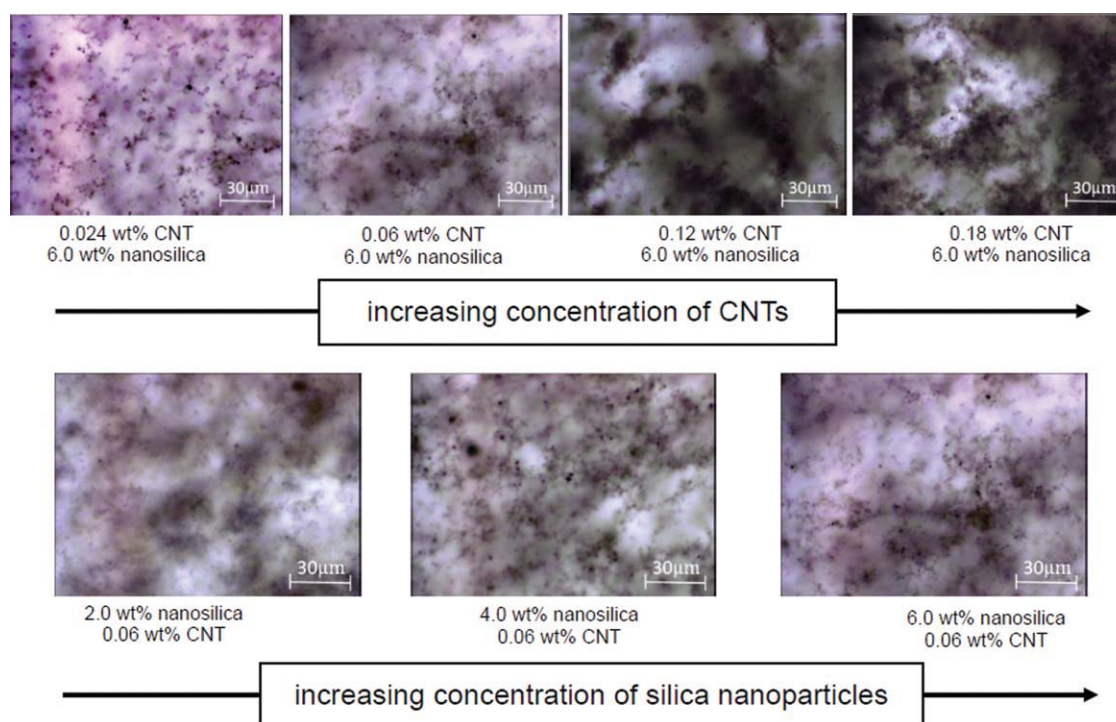


**Figure 2** Transmission optical microscopy images of the nanocomposites with various concentrations of silica nanoparticles and MWCNTs. [Color figure can be viewed in the online issue, which is available at [wileyonlinelibrary.com](http://wileyonlinelibrary.com).]

between 142 and 147°C with no clear trend for the different formulations being apparent. These values are in good agreement with previously published data for the silica nanoparticle-modified epoxy.<sup>15</sup> Thus, the results shown in Table I reveal that the presence of these nanoscale inorganic modifiers does not significantly affect the  $T_g$  of the nanocomposites.

#### Fracture toughness of the nanocomposites

The values of the fracture toughness,  $K_C$ , and the fracture energy,  $G_C$ , of the unmodified epoxy poly-

mer and the nanocomposites are given in Table II. The values of  $G_C$  are also shown graphically in Figure 4.

The addition of the silica nanoparticles alone leads to a significant increase in the fracture energy,  $G_C$ , for the nanocomposites. For example, the incorporation of 6.0 wt % of silica nanoparticles gives a 36% increase in  $G_C$  compared with the unmodified epoxy polymer. The values of the fracture toughness,  $K_C$ , increase somewhat less as these variables are related by  $G_C = (1 - \nu^2)(K_C)^2/E$ , where  $\nu$  is the Poisson's

**TABLE I**  
Formulations, Young's Moduli, and Glass Transition Temperatures of the Nanocomposites

| Silica nanoparticles (wt %) | MWCNTs (wt %) | Young's modulus, $E$ (GPa) |      | $T_g$ (°C) |     |
|-----------------------------|---------------|----------------------------|------|------------|-----|
|                             |               | Mean                       | ±    | Mean       | ±   |
| 0.0                         | 0.00          | 2.90                       | 0.05 | 146.8      | 0.9 |
| 2.0                         | 0.00          | 2.95                       | 0.02 | 145.6      | 1.5 |
|                             | 0.06          | 2.95                       | 0.05 | 144.0      | 1.3 |
| 4.0                         | 0.00          | 3.00                       | 0.07 | 146.2      | 0.9 |
|                             | 0.06          | 3.00                       | 0.05 | 145.0      | 2.2 |
|                             | 0.12          | 3.04                       | 0.07 | 146.1      | 1.0 |
| 6.0                         | 0.00          | 3.01                       | 0.06 | 143.4      | 0.7 |
|                             | 0.02          | 3.00                       | 0.06 | 145.1      | 1.1 |
|                             | 0.06          | 3.03                       | 0.06 | 142.3      | 2.0 |
|                             | 0.12          | 3.04                       | 0.04 | 143.2      | 0.9 |
|                             | 0.18          | 3.04                       | 0.03 | 144.2      | 1.2 |

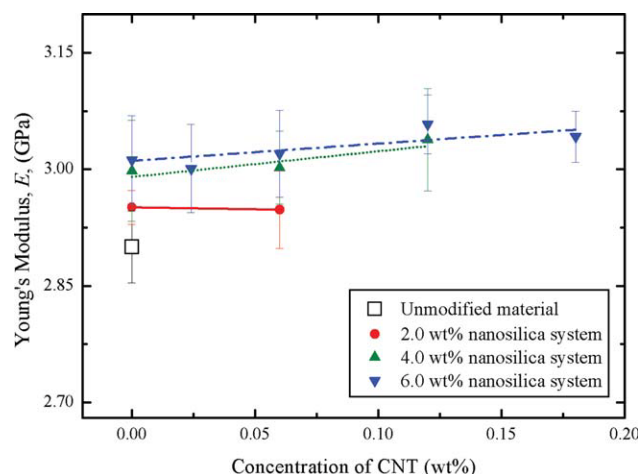


**Figure 3** Young's moduli of the nanocomposites containing silica nanoparticles and MWCNTs as a function of the concentration of MWCNTs.

**TABLE II**  
Fracture Toughness and Fracture Energy of the Nanocomposites

| Silica nanoparticles (wt %) | MWCNTs (wt %) | Fracture toughness, $K_C$ (MPam <sup>1/2</sup> ) |      | Fracture energy, $G_C$ (J/m <sup>2</sup> ) |    |
|-----------------------------|---------------|--|------|--|----|
|                             |               | Mean   | ±    | Mean                                       | ±  |
| 0.0                         | 0.00          | 0.69   | 0.04 | 133  | 8  |
| 2.0                         | 0.00          | 0.68   | 0.03 | 152  | 16 |
|                             | 0.06          | 0.75   | 0.02 | 176  | 17 |
| 4.0                         | 0.00          | 0.72   | 0.08 | 171  | 23 |
|                             | 0.06          | 0.88   | 0.05 | 187  | 23 |
| 6.0                         | 0.12          | 0.91   | 0.06 | 192  | 20 |
|                             | 0.00          | 0.75   | 0.03 | 181  | 15 |
|                             | 0.02          | 0.83   | 0.13 | 193  | 8  |
|                             | 0.06          | 0.96   | 0.12 | 195  | 17 |
|                             | 0.12          | 0.99   | 0.10 | 199  | 12 |
|                             | 0.18          | 1.03   | 0.10 | 204  | 19 |

ratio.<sup>26</sup> The increase in modulus because of the addition of silica is relatively small and would reduce  $G_C$  if  $K_C$  was constant.

In contrast, the further addition of the MWCNTs, to form hybrid nanocomposites, leads to a significant increase in the fracture toughness,  $K_C$ , of between 22 and 28% when a relatively low concentration of 0.06 wt % MWCNTs is incorporated into the hybrid nanocomposites, which also contain 4.0 and 6.0 wt % silica nanoparticles. As may be seen when the values of  $K_C$  for these hybrid nanocomposite formulations are compared to the formulations containing only the silica nanoparticles. Further, when compared with the unmodified epoxy polymer, an increase of between 28 and 39% in the value of the fracture toughness,  $K_C$ , is obtained for the hybrid nanocomposites. However, upon increasing the concentration of MWCNTs to greater than 0.06 wt %, then there is no significant further increase in the value of the fracture toughness. A maximum value of fracture toughness,  $K_C$ , of 1.03 MPam<sup>1/2</sup> is recorded at 6.0 wt % silica nanoparticles and 0.18 wt % MWCNTs, and this value of  $K_C$  is 49% higher than that of the unmodified epoxy polymer. The results of the fracture energy,  $G_C$ , are shown in Table II and Figure 4 and indicate that the maximum improvement of the value of  $G_C$  again occurs for the hybrid nanocomposite containing 6.0 wt % silica nanoparticles and 0.18 wt % MWCNTs, and the value of  $G_C$  for this formulation is 53% higher than that of the unmodified epoxy polymer.

The increases in fracture energy measured in this work, to a maximum of 204 J/m<sup>2</sup>, are relatively small compared to those that may be obtained using rubber particles. For example, Hsieh et al.<sup>15</sup> used a carboxyl-terminated butadiene-acrylonitrile (CTBN) rubber and obtained a  $G_C$  of 671 J/m<sup>2</sup> with an addition of 9 wt % in the same epoxy polymer. However, the modulus and  $T_g$  were also reduced.

### Morphology of the fracture surfaces

To examine the toughening mechanisms that can contribute to the increases in the toughness of the nanocomposites reported above, a FEG-SEM was used to examine the fracture surfaces of the failed SENB specimens.

The fracture surface of the nanocomposite incorporating 6.0 wt % silica nanoparticles and 0.18 wt % MWCNTs is shown in Figure 5. In Figure 5(a), the well-established mechanism of nanotube pull-out<sup>27,28</sup> can be clearly observed and is labeled. By analyzing the number of such pulled-out CNTs on the fracture surface, using image analysis software, it was found that ~ 1.5% of the nanotubes underwent pull-out. The nanotube pull-out mechanism includes the energy contributions from the sliding friction occurring at the interface between the CNTs and the epoxy polymer, followed by nanotube rupture; the pulled-out length can be up to ~ 0.5 μm, see Figure 5(a). Both of these energy-dissipative contributions may lead to an improvement in the toughness of the nanocomposite. In the higher magnification image, see Figure 5(b), voids around the CNTs may be seen. These voids arise from debonding between the MWCNTs and the epoxy polymer, which is followed by plastic deformation of the epoxy. In addition, some voids form in the agglomerates of the MWCNTs, as may be seen in Figure 5(c). As the formation of these voids involves plastic deformation of the epoxy polymer, the toughness of the nanocomposite is enhanced. (It should be noted that the AFM images of the initial morphology of the nanocomposites showed no voids within the MWCNT agglomerates, indicating that these are a feature of the fracture process, rather than a manufacturing defect. Also, new surface area created by the debonding mechanism will dissipate strain energy,

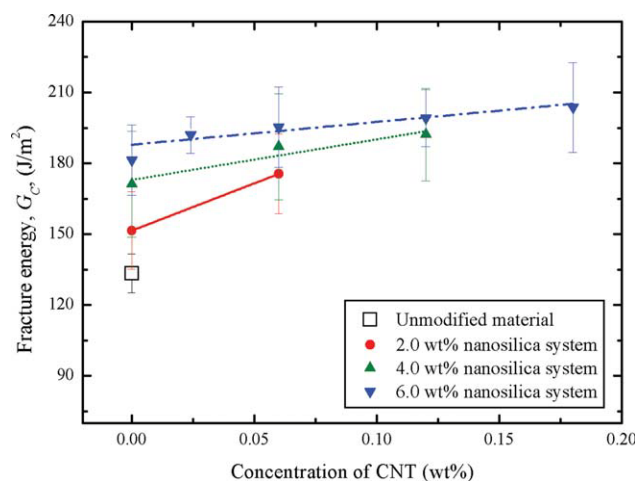


**Figure 4** The fracture energy,  $G_C$ , of the nanocomposites containing silica nanoparticles and MWCNTs as a function of the concentration of MWCNTs.



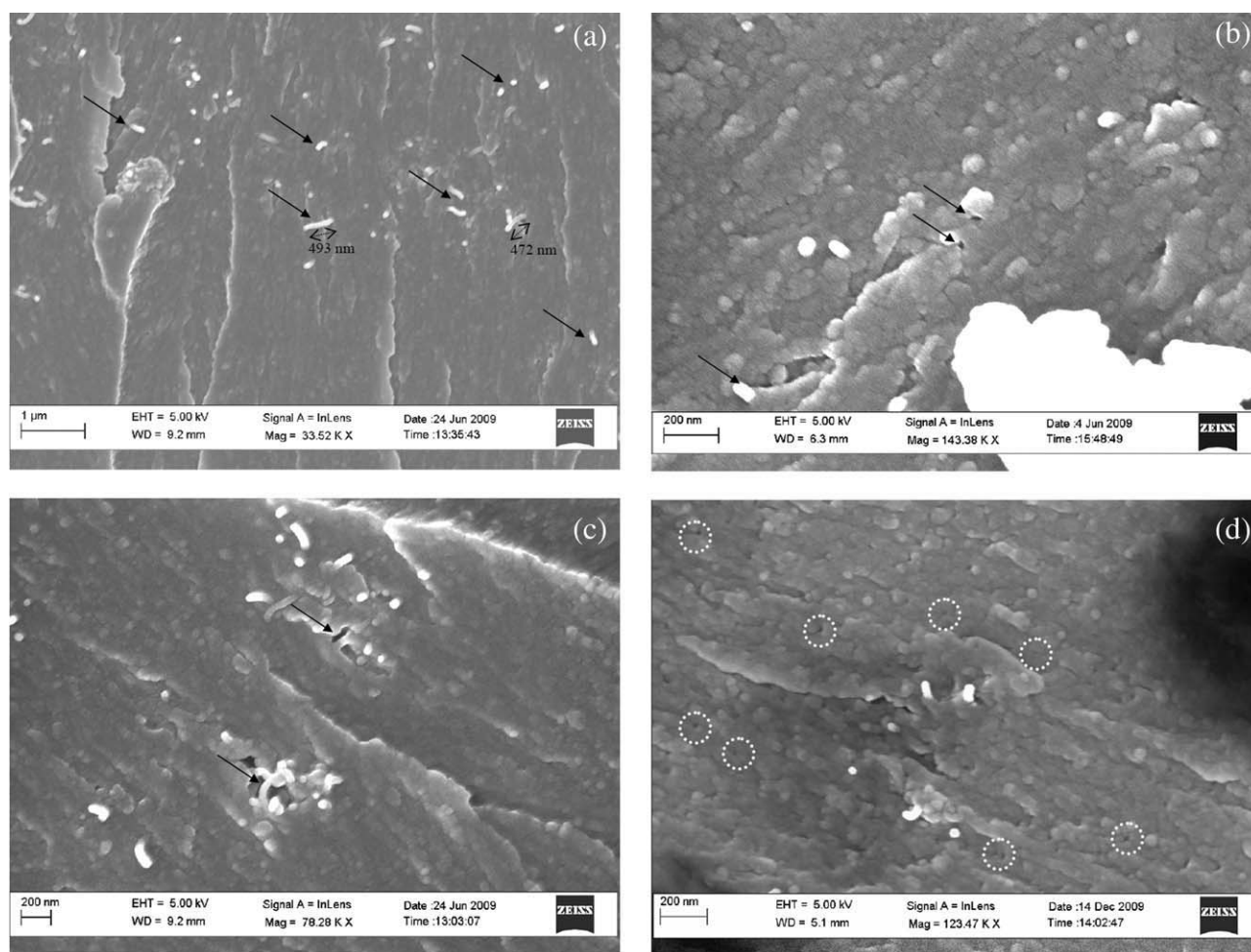


**Figure 5** FEG-SEM images of the nanocomposite containing 6.0 wt % silica nanoparticles and 0.18 wt % MWCNTs, showing (a) pulled-out CNTs, (b) voids associated with the CNTs, (c) voids within the CNT agglomerates, and (d) voids associated with the silica nanoparticles.

although this contribution is considered to be relatively minor.<sup>15)</sup>

The toughening mechanisms caused by the presence of silica nanoparticles can be clearly identified in a high-resolution image, as shown in Figure 5(d), in which the occurrence of plastic void growth after debonding of the silica particles from the epoxy polymer can be readily observed. This toughening mechanism of void initiation and growth associated with the silica nanoparticles has been described, and quantitatively modeled, in a previous study.<sup>15)</sup>

## CONCLUSIONS

Silica nanoparticles and MWCNTs have been incorporated into an anhydride-cured epoxy resin to form “hybrid” nanocomposites. A good dispersion of the silica nanoparticles was found to occur, even at relatively high concentrations of the nanoparticles. However, in contrast, the MWCNTs were not so well dispersed but relatively agglomerated.

The glass transition temperature of the epoxy polymer was 145°C and was unaffected by the addition of the silica nanoparticles or the MWCNTs. The Young’s modulus was increased by the addition of the silica nanoparticles, but the addition of up to 0.18 wt % MWCNTs had no further significant effect.

The addition of silica nanoparticles alone led to a significant increase in the fracture energy,  $G_C$ , for the nanocomposites. For example, the incorporation of 6.0 wt % of silica nanoparticles gave a 36% increase in  $G_C$  compared with the unmodified epoxy polymer. The further addition of the MWCNTs, to form hybrid nanocomposites, led to a further increase in the fracture energy. A maximum  $G_C$  of 204 J/m<sup>2</sup> was recorded at 6.0 wt % silica nanoparticles and 0.18 wt % MWCNTs, which is 53% higher than that of the unmodified epoxy polymer.

The toughening mechanisms that cause such enhancements of the toughness of the hybrid nanocomposites have been identified. They involve pull-out of the CNTs and void initiation and growth,

which involves plastic deformation of the epoxy polymer, associated with both the presence of the silica nanoparticles and the MWCNTs.

The authors thank Nanoledge and Nanoresins for the supply of materials. Some of the equipment used was provided by Dr. Taylor's Royal Society Mercer Junior Award for Innovation.

## References

1. Kinloch, A. J.; Shaw, S. J.; Tod, D. A.; Hunston, D. L. *Polymer* 1983, 24, 1341.
2. Yee, A. F.; Pearson, R. A. *J Mater Sci* 1986, 21, 2462.
3. Bucknall, C. B.; Partridge, I. K. *Polymer* 1983, 24, 639.
4. Johnsen, B. B.; Kinloch, A. J.; Taylor, A. C. *Polymer* 2005, 46, 7352.
5. Kinloch, A. J.; Taylor, A. C. *J Mater Sci* 2006, 41, 3271.
6. Broutman, L. J.; Sahu, S. *Mater Sci Eng* 1971, 8, 98.
7. Johnsen, B. B.; Kinloch, A. J.; Mohammed, R. D.; Taylor, A. C.; Sprenger, S. *Polymer* 2007, 48, 530.
8. Kinloch, A. J.; Mohammed, R. D.; Taylor, A. C.; Eger, C.; Sprenger, S.; Egan, D. *J Mater Sci* 2005, 40, 5083.
9. Zilg, C.; Mulhaupt, R.; Finter, J. *Macromol Chem Phys* 1999, 200, 661.
10. Shaffer, M. S. P.; Kinloch, I. A. *Compos Sci Technol* 2004, 64, 2281.
11. Yeh, M. K.; Hsieh, T. H.; Tai, N. H. *Mater Sci Eng A* 2008, 483, 289.
12. Yeh, M. K.; Hsieh, T. H. *Compos Sci Technol* 2008, 68, 2930.
13. Zhang, W.; Picu, R. C.; Koratkar, N. *Appl Phys Lett* 2007, 91, 193109.
14. Singh, R. P.; Zhang, M.; Chan, D. *J Mater Sci* 2002, 37, 781.
15. Hsieh, T. H.; Kinloch, A. J.; Masania, K.; Sohn Lee, J.; Taylor, A. C.; Sprenger, S. *J Mater Sci* 2010, 45, 1193.
16. Iijima, S. *Nature* 1991, 354, 56.
17. Xie, S.; Li, W.; Pan, Z.; Chang, B.; Sun, L. *J Phys Chem Solids* 2000, 61, 1153.
18. Falvo, M. R.; Clary, G. J.; Taylor, R. M.; Chi, V.; Brooks, F. P.; Washburn, S.; Superfine, R. *Nature* 1997, 389, 582.
19. Bai, J. *Carbon* 2003, 41, 1325.
20. Wong, M.; Paramsothy, M.; Xu, X. J.; Ren, Y.; Li, S.; Liao, K. *Polymer* 2003, 44, 7757.
21. Gojny, F. H.; Wichmann, M. H. G.; Kopke, U.; Fiedler, B.; Schulte, K. *Compos Sci Technol* 2004, 64, 2363.
22. BS-ISO-11357-2. *Plastics—Differential Scanning Calorimetry (DSC)—Part 2: Determination of Glass Transition Temperature*; BSI: London, 1999.
23. ASTM-D638. *Standard Test Method for Tensile Properties of Plastics*; ASTM: West Conshohocken, 2008.
24. ASTM-D5045. *Standard Test Method for Plane-Strain Fracture Toughness and Strain-Energy Release Rate of Plastic Materials*; ASTM: West Conshohocken, 2007.
25. BS-ISO-13586. *Plastics—Determination of Fracture Toughness ( $G_{IC}$  and  $K_{IC}$ )—Linear Elastic Fracture Mechanics (LEFM) Approach*; BSI: London, 2000.
26. Kinloch, A. J. *Adhesion and Adhesives: Science and Technology*; Chapman & Hall: London, 1987.
27. Gojny, F. H.; Wichmann, M. H. G.; Fiedler, B.; Schulte, K. *Compos Sci Technol* 2005, 65, 2300.
28. Wichmann, M. H. G.; Schulte, K.; Wagner, H. D. *Compos Sci Technol* 2008, 68, 329.